

FootSLAM meets Adaptive Thresholding

Johan Wahlström, Andrew Markham, and Niki Trigoni

Abstract—Calibration of the zero-velocity detection threshold is an essential prerequisite for zero-velocity-aided inertial navigation. However, the literature is lacking a self-contained calibration method, suitable for large-scale use in unprepared environments without map information or pre-deployed infrastructure. In this paper, the calibration of the zero-velocity detection threshold is formulated as a maximum likelihood problem. The likelihood function is approximated using estimation quantities readily available from the FootSLAM algorithm. Thus, we obtain a method for adaptive thresholding that does not require map information, measurements from supplementary sensors, or user input. Experimental evaluations are conducted using data with different gait speeds, sensor placements, and walking trajectories. The proposed calibration method is shown to outperform fixed-threshold zero-velocity detectors.

Index Terms—FootSLAM, SLAM, adaptive thresholding, inertial navigation, zero-velocity updates, indoor positioning.

I. INTRODUCTION

Zero-velocity-aided inertial navigation has been hailed as one of the most promising technologies for indoor positioning in environments without pre-installed infrastructure or prior map information. Consider, for example, firefighters arriving at an emergency scene with low visibility, intense heat, scattered debris and building materials, and no general knowledge of the area. In this situation, zero-velocity-aided inertial navigation provides a reliable, low-cost positioning solution with no setup time and no dependence on environmental conditions such as visibility or obstacles in line-of-sight [1], [2].

The performance of a zero-velocity-aided inertial navigation system is highly dependent on the design and calibration of the zero-velocity detector. Typically, the detector is implemented as a generalized likelihood ratio test; the sensor unit is considered to be stationary if the likelihood ratio exceeds a user-specified threshold [3]. If the threshold on the likelihood ratio is too large, the detector will not be able to detect stationary instances when the user is running. If the threshold is too small, the detector will produce false zero-velocity instances. In addition, the optimal threshold will be dependent on factors such as gait technique, the placement of the sensor, the type of shoe, and the walking surface.

Adaptive thresholding has been explored in several studies [4]–[11]. Often, the threshold is set based on the result of a speed or motion mode classification. However, the predefined threshold values, associated with the respective motion modes, need to be calibrated using ground truth position data. Since

This research has been financially supported by the National Institute of Standards and Technology (NIST) via the grant *Pervasive, Accurate, and Reliable Location-based Services for Emergency Responders* (Federal Grant: 70NANB17H185).

J. Wahlström, A. Markham and N. Trigoni are with the Department of Computer Science, University of Oxford, Oxford, UK ({johan.wahlstrom, andrew.markham, niki.trigoni}@cs.ox.ac.uk).

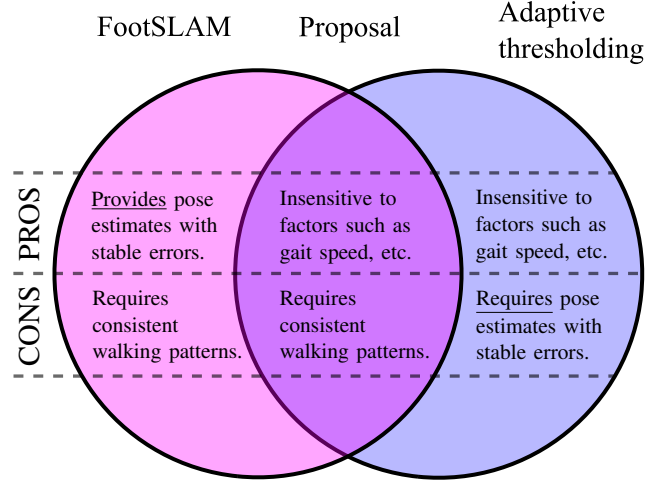


Fig. 1. A Venn diagram illustrating the relation between FootSLAM, previous methods for adaptive thresholding, and our proposal.

such data is not available in unprepared environments, this means that current implementations of adaptive thresholding require an extensive calibration period – separate from the real-world deployment for which the navigation system is intended – and that the threshold values, once set, cannot adapt to real-time changes in gait or environment conditions that were not accounted for in the calibration process.

As illustrated in Fig. 1, the problem of calibrating the zero-velocity detection threshold is in this paper approached via the FootSLAM algorithm. FootSLAM is a method for transforming odometry with position drift into pose estimates with long-term error stability. Thus, the calibration can be performed by treating the output from FootSLAM as a pseudo ground truth. The calibration algorithm is formulated as the solution to a maximum likelihood problem, and the likelihood function is approximated using particle weights produced by FootSLAM. In this way, a joint calibration and navigation algorithm that is completely independent of any supplementary ground truth data is obtained. The method is validated using a diverse set of experimental data.

Sections II and III review previous work on adaptive thresholding and FootSLAM, respectively. Section IV describes the proposed algorithm. Experimental results are presented in Section V and the article is concluded in Section VI.

II. INERTIAL ODOMETRY AND ADAPTIVE THRESHOLDING

The purpose of a zero-velocity-aided inertial navigation system (INS) is to compute the odometry estimates

$$\mathbf{z}_{1:T} = \mathcal{G}_\theta(\mathbf{y}_{1:T}). \quad (1)$$

Here, \mathbf{z}_k denotes an estimate of the three-dimensional translation and rotation of the inertial sensors between sampling

instances $k - 1$ and k . Further, \mathbf{y}_k denotes the inertial measurements at sampling instance k , $\mathbf{y}_{1:T} \triangleq \{\mathbf{y}_1, \dots, \mathbf{y}_T\}$, and the transformation $\mathcal{G}_\theta(\cdot)$ is a filter or smoother composed of the navigation equations and a zero-velocity detector with the zero-velocity detection threshold θ . The transformation $\mathcal{G}_\theta(\cdot)$ is dependent on several design parameters, including initialization parameters, parameters characterizing sensor errors, and parameters used by the zero-velocity detector. However, we will, in similarity with previous studies on parameter estimation for zero-velocity-aided INSs, primarily focus on the tuning of the zero-velocity detection threshold [4]–[10]. The optimal threshold value may vary with a large number of factors, and an improper tuning can have a detrimental effect on performance.

To find a suitable threshold, one must typically make use of ground truth data in the form of maps, user provided location information, or measurements from complementary sensors. A common approach is to first estimate or classify the speed or motion mode of the user. Based on the result, the detector selects a threshold value that has been optimized, using ground truth data, for that specific speed or motion class [4]–[9]. However, other calibration methods have also been proposed. In [10], a time-varying threshold was obtained by formulating the likelihood ratio test in a Bayesian setting; in [12], the threshold was set based on the variance of the accelerometer measurements computed over a specified time window; and in [13], the threshold was fixed while instead varying the window length of the samples used to compute the detection statistic. There have also been attempts at designing robust zero-velocity detectors by using neural networks [14], by incorporating velocity estimates into the detector [15], [16], or by inferring the state of gait cycle [17], [18].

III. FOOTSLAM

The idea of FootSLAM is to represent a two-dimensional navigation area using a grid of hexagons, and then learn the probability of transitioning from a given hexagon to an adjacent one [19]. This is illustrated in Fig. 2. The inference framework utilizes the Rao-Blackwellized particle filtering approach of the FastSLAM algorithm. Thus, the posterior $p(\mathbf{x}_{0:T}, \mathbf{m} | \mathbf{z}_{1:T})$ is factorized as

$$p(\mathbf{x}_{0:T}, \mathbf{m} | \mathbf{z}_{1:T}) = \underbrace{p(\mathbf{m} | \mathbf{x}_{0:T})}_{\text{map estimation}} \cdot \underbrace{p(\mathbf{x}_{0:T} | \mathbf{z}_{1:T})}_{\text{pose estimation}} \quad (2)$$

where \mathbf{x} and \mathbf{m} represent the pose and map, respectively, with \mathbf{z}_k treated as a noisy measurement of the difference between \mathbf{x}_{k-1} and \mathbf{x}_k . The pose is recursively estimated according to

$$p(\mathbf{x}_{0:k} | \mathbf{z}_{1:k}) \propto \underbrace{p(\mathbf{z}_k | \mathbf{x}_{k-1:k})}_{\text{likelihood}} \underbrace{p(\mathbf{x}_k | \mathbf{x}_{0:k-1})}_{\text{pose transition}} \underbrace{p(\mathbf{x}_{0:k-1} | \mathbf{z}_{1:k-1})}_{\text{previous posterior}} \quad (3)$$

The likelihood function $p(\mathbf{z}_k | \mathbf{x}_{k-1:k})$ is used to draw samples of \mathbf{x}_k , whereas the pose transition probability $p(\mathbf{x}_k | \mathbf{x}_{0:k-1})$, which is computed by marginalizing over the map, is used in the particle weight update

$$w_k^{(i)} \propto p(\mathbf{x}_k^{(i)} | \mathbf{x}_{0:k-1}^{(i)}) w_{k-1}^{(i)} \quad (4)$$

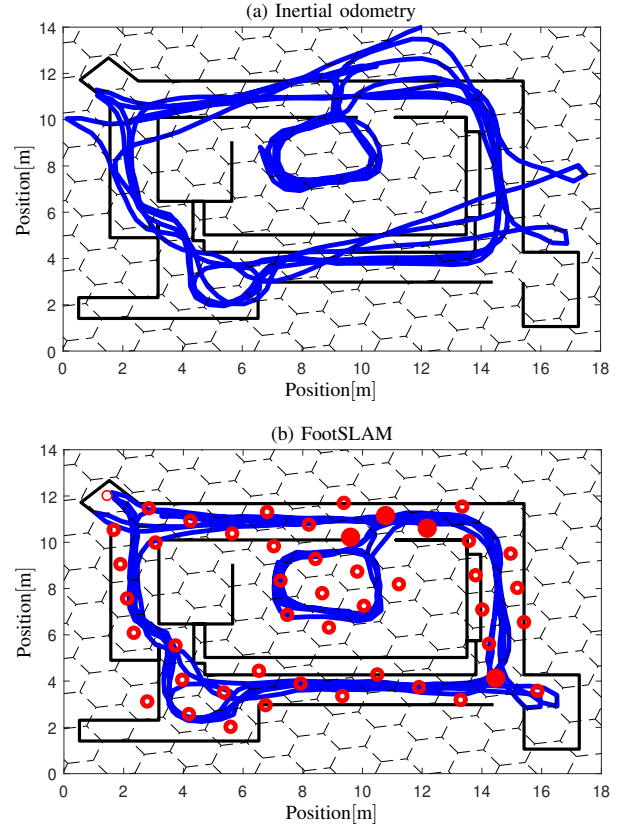


Fig. 2. Illustration of (a) stand-alone zero-velocity-aided inertial navigation and (b) FootSLAM after about four minutes of walking in an office building. The sizes of the red circles in (b) indicate the prevalence of transitions involving the associated hexagons.

where $w^{(i)}$ denotes the weight of the i th particle. The pose transition probability is large when $\mathbf{x}_{k-1} \rightarrow \mathbf{x}_k$ or $\mathbf{x}_k \rightarrow \mathbf{x}_{k-1}$ corresponds to a frequently observed hexagon transition, and the filter will thus favor particles that revisit the same hexagon transitions (and thereby outline consistent walking patterns). However, note that without any absolute heading, position, or scale information, the estimates are invariant under rotation, translation, and scaling of the odometry in the plane.

Finally, the navigation solution is represented by a set of pose estimates $\{\{\mathbf{x}_k^{(i)}\}_{i=1}^N\}_{k=0}^T$ and associated weights $\{\{w_k^{(i)}\}_{i=1}^N\}_{k=0}^T$, where N is the number of particles. Extensions of the FootSLAM algorithm have considered estimation of systematic odometry errors [19], navigation and mapping in three dimensions [20], collaborative mapping [21], fusion with magnetic field measurements [22] and user provided hints [23], and navigation in the presence of moving platforms such as escalators and elevators [24].

IV. ADAPTIVE THRESHOLDING USING FOOTSLAM

The maximum likelihood estimate of the threshold is

$$\hat{\theta} = \arg \max_{\theta} p_{\theta}(\mathbf{y}_{1:T}) \quad (5)$$

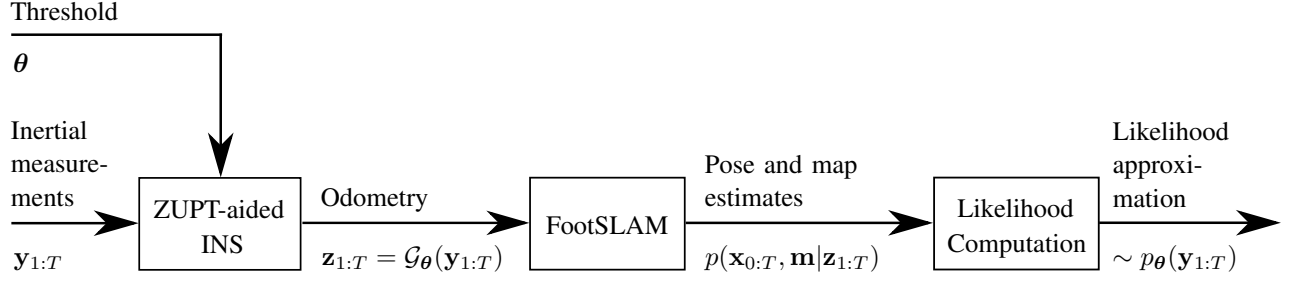


Fig. 3. System overview. The FootSLAM algorithm is fed with odometry from a zero-velocity-aided inertial navigation system. The likelihood is approximated using estimates provided by FootSLAM.

where the likelihood function can be approximated as

$$\begin{aligned}
 p_\theta(y_{1:T}) &\approx p(z_{1:T}) \\
 &= \prod_{k=1}^T p(z_k | z_{1:k-1}) \\
 &= \prod_{k=1}^T \int p(z_k | \mathbf{x}_{k-1:k}) p(\mathbf{x}_k | \mathbf{x}_{0:k-1}) \\
 &\quad \cdot p(\mathbf{x}_{0:k-1} | z_{1:k-1}) d\mathbf{x}_{0:k} \\
 &\approx \prod_{k=1}^T \sum_{i=1}^N p(\mathbf{x}_k^{(i)} | \mathbf{x}_{0:k-1}^{(i)}) w_{k-1}^{(i)}
 \end{aligned} \quad (6)$$

and we use the convention that $z_{1:0} = \emptyset$. The first approximation in (6) corresponds to approximations made in the nonlinear system for zero-velocity-aided inertial navigation and when only using the point estimates of the odometry, whereas the second approximation is a conventional particle filter approximation [25].

The result in (6) demonstrates that the value of the likelihood function for a given threshold can be approximated based on the output obtained from FootSLAM when using the same threshold to compute the odometry. In particular, comparing with (4), we see that the likelihood approximation in (6) uses the sum of the particle weights *before* normalization. Thus, as should be intuitive, the likelihood function is large when $p(\mathbf{x}_k^{(i)} | \mathbf{x}_{0:k-1}^{(i)})$ tends to be large, i.e., when the particles are prone to make repeated hexagon transitions.

By utilizing the recursion

$$p_\theta(y_{1:k}) \approx p_\theta(y_{1:k-1}) \cdot \sum_{i=1}^N p(\mathbf{x}_k^{(i)} | \mathbf{x}_{0:k-1}^{(i)}) w_{k-1}^{(i)} \quad (7)$$

with the initialization $p_\theta(y_{1:0}) = 1$, the value of the likelihood function can be updated after each time step in the FootSLAM algorithm, and there's no need to store all pose and map estimates produced by FootSLAM. Further, note that the likelihood value can be computed online by updating the zero-velocity-aided INS, the FootSLAM algorithm, and the likelihood estimates after obtaining each new sample of inertial measurements. The relation between zero-velocity-aided inertial navigation, FootSLAM, and the likelihood computation is illustrated in Fig. 3. In the end, we find an approximate maximum likelihood estimate by performing a grid search over a specified set of threshold values. The method for estimating the threshold is summarized in Algorithm 1.

V. EXPERIMENTAL RESULTS

The proposed method was evaluated in two separate experiments. The experiments demonstrate calibration during

Algorithm 1: Maximum likelihood estimation of the zero-velocity detection threshold.

Input: Inertial measurements $y_{1:T}$.

Output: Threshold estimate $\hat{\theta}$.

- 1) Specify a set of thresholds $\{\theta^{(1)}, \dots, \theta^{(M)}\}$. For $j = 1, \dots, M$:
 - a) Compute the odometry $z_{1:T}$ by applying a zero-velocity-aided inertial navigation system with the threshold $\theta^{(j)}$ to the inertial measurements $y_{1:T}$.
 - b) Run FootSLAM on the odometry $z_{1:T}$ and approximate $p_{\theta^{(j)}}(y_{1:T})$ using (7).
 - 2) Choose the estimate as the threshold that produced the largest value of the likelihood function.
-

both repetitive walking along a marked trajectory and during day-to-day walking in an office environment. In addition, we considered several different gait speeds and sensor placements. Inertial measurements were collected at a sampling rate of 100 [Hz] from a Xsens MTi-3-8A7G6-DK IMU. The odometry was computed using a Kalman smoother [26], implemented with the stance hypothesis optimal detection (SHOE) zero-velocity-detector [3]. The yaw rate bias was included as a state element in the FootSLAM algorithm [23], and the particles were resampled using systematic resampling [27]. *The data and the code used in the experiments are available at <https://www.cs.ox.ac.uk/people/johan.wahlstrom/>.*

A. Closed-loop Trajectory with Speed Variations

In the first experiment, calibration and evaluation data were collected for three gait modes: walking, fast walking, and jogging, with average speeds of about 4.5 [km/h], 6.5 [km/h], and 8 [km/h], respectively. The sensor was placed on top of the shoelaces as illustrated by placement a) in Fig. 4. All data was recorded while walking or jogging along a rectangle of dimensions 2.6 [m] \times 3.2 [m]. For each gait mode, we collected i) calibration data consisting of one data recording of ten consecutive laps, and ii) evaluation data consisting of 50 data recordings of one lap each. Fig. 5 (a) displays the position RMSEs for the three gait modes, computed using the initial



Fig. 4. Illustration of the sensor placements a) 'Shoelaces', b) 'Ankle', c) 'Heel', and d) 'Toes'.

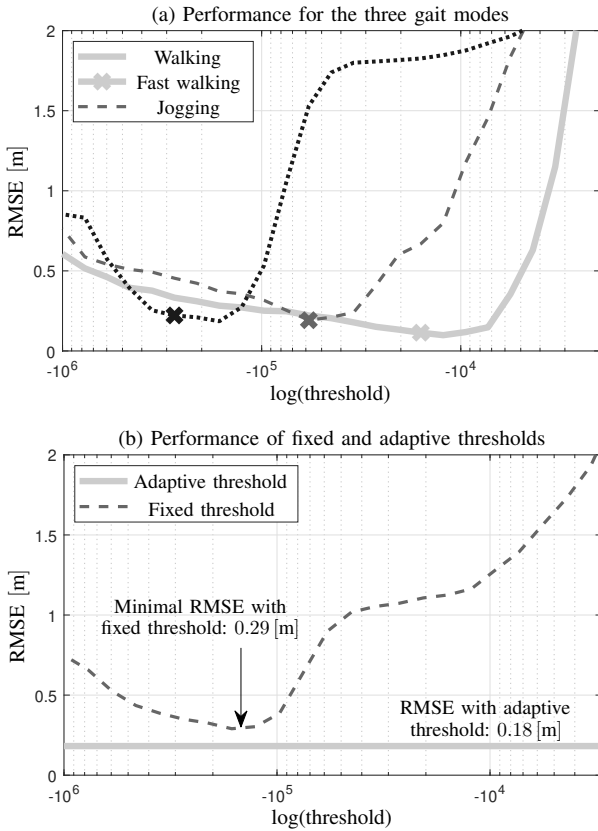


Fig. 5. Position error of a zero-velocity aided inertial navigation system after walking along a closed-loop trajectory with a length of about twelve meters. The crosses in a) indicate the thresholds chosen by the calibration algorithm. Three gait modes were used: walking, fast walking, and jogging.

and final position estimates in each recording in the evaluation data (all recordings started and ended at the same position).

For each gait mode, the calibration data was used to estimate the threshold as described in Section IV. The evaluation data was then used to compare the performance of i) a zero-velocity-aided INS using, for each gait mode, the threshold estimate found using the calibration data, and ii) a zero-velocity-aided INS using the same threshold for all gait modes. The resulting horizontal position RMSEs are shown in Fig. 5

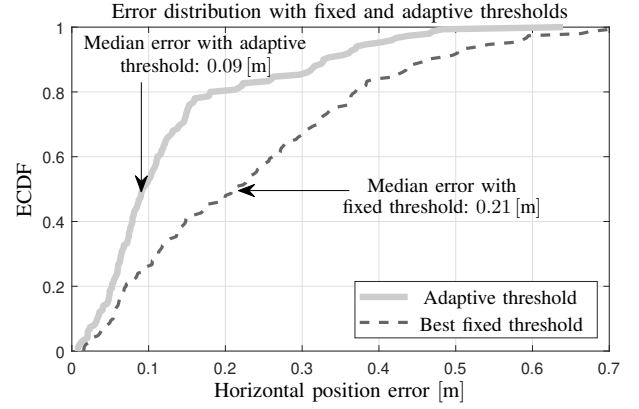


Fig. 6. Empirical cumulative distribution functions of position errors after walking along a closed-loop trajectory with a length of about twelve meters. Three gait modes were used: walking, fast walking, and jogging.

(b)¹. As can be seen, the adaptive threshold performs significantly better than the best fixed threshold. Fig. 6 compares the adaptive threshold with the best (in terms of RMSE) fixed threshold, by displaying the empirical cumulative distribution functions (ECDF) of the horizontal position error. In comparison with the best fixed threshold, the adaptive threshold reduces the median horizontal position error by more than 50%. When concatenating all evaluation data into a single trajectory of length 1.74 [km], the norm of the horizontal position error of the adaptive threshold and best fixed threshold becomes 16.58 [m] and 31.48 [m], respectively.

B. Office Environment with Different Sensor Placements

In the second experiment, calibration and evaluation data were recorded using the three sensor placements 'Ankle', 'Heel', and 'Toes', illustrated in Fig. 4. The gait speed was around 6 [km/h]. The calibration data was recorded while walking in an office environment of about 200 [m²]. The pedestrian started at the entrance door and then walked for about three minutes in between his personal desk, a meeting room, a kitchen, a lab room, a printer, and a bathroom. The trajectory is illustrated in Fig. 7. The evaluation data was recorded in the same way as in the first experiment. Fig. 8 (a) displays the resulting position RMSEs for the three sensor placements. As seen from Figs. 8 (b) and 9, the adaptive threshold gives a slight performance improvement in comparison with the best fixed threshold. However, when interpreting these results, note that the two sensor placements 'Heel' and 'Toes' perform well for a wide range of thresholds. As a result, even an optimal choice of threshold (in terms of RMSE) for each sensor placement would only improve the RMSE by about one and a half centimeter in comparison with the best fixed threshold. When merging all evaluation data, the norm of the horizontal position error of the adaptive threshold and best fixed threshold becomes 13.16 [m] and 14.03 [m], respectively. The position errors obtained when concatenating all evaluation into a single trajectory is summarized in Table I.

¹Note that the horizontal axis displays the value of the fixed threshold. Thus, the RMSE for the adaptive threshold, which is not dependent on the fixed threshold, is shown as a horizontal line.

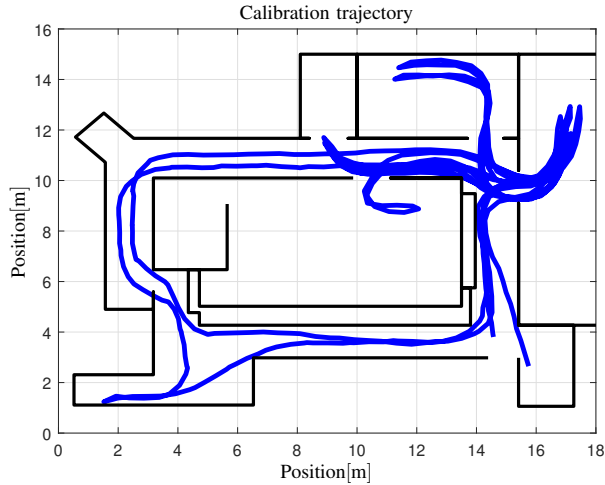


Fig. 7. Trajectory used for calibration in office environment.

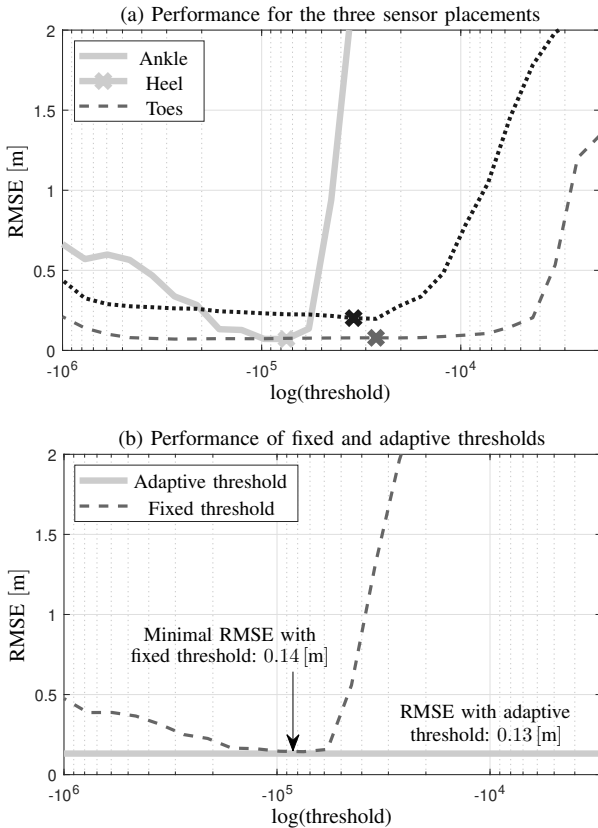


Fig. 8. Position error of a zero-velocity aided inertial navigation system after walking along a closed-loop trajectory with a length of about twelve meters. The crosses in a) indicate the thresholds chosen by the calibration algorithm. The data was recorded using the three sensor placements ‘Ankle’, ‘Heel’, and ‘Toes’, illustrated in Fig. 4.

VI. SUMMARY AND DISCUSSION

This paper has demonstrated the complementary benefits of two research directions – FootSLAM and adaptive thresholding – that for a long period of time has developed separately. There are two problems with established methods for adaptive thresholding. Firstly, they need to be trained using large sets of data. Secondly, they can typically only adjust to variations

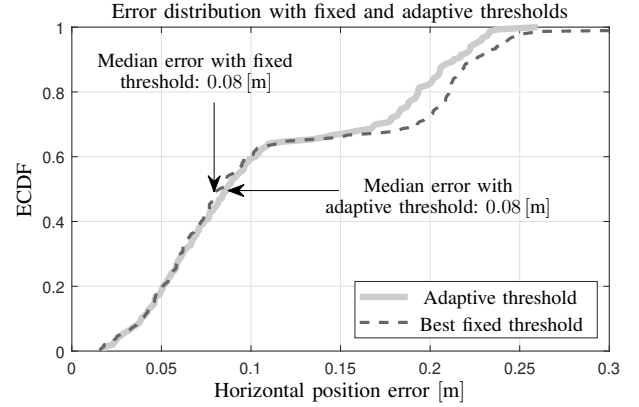


Fig. 9. Empirical cumulative distribution functions of position errors after walking along a closed-loop trajectory with a length of about twelve meters. The data was recorded using the three sensor placements ‘Ankle’, ‘Heel’, and ‘Toes’, illustrated in Fig. 4.

TABLE I
NORM OF POSITION ERROR AFTER MERGING ALL EVALUATION DATA.

Varying factor	Threshold	
	Adaptive	Best fixed
Gait speed	16.58 [m]	31.48 [m]
Sensor placement	13.16 [m]	14.03 [m]

in speed or gait mode, and not to variations in for example the walking surface or the sensor placement. However, by calibrating a zero-velocity-aided INS using the position estimates provided by FootSLAM, it is possible to solve both of these problems. Specifically, we have presented a maximum likelihood-based algorithm for adaptive thresholding that is completely independent of ground truth data or additional information. The adaptive detector was shown to outperform detectors with fixed thresholds on data with different gait speeds and sensor placements. In the former case, the median horizontal position error was reduced by more than 50%.

The only price to pay for not relying on ground truth data is that the FootSLAM algorithm needs to converge during the calibration period. In other words, there needs to be a period of time with consistent (in terms of hexagon transitions) walking patterns. However, as supported by the large number of publications on the FootSLAM algorithm, physical constraints provided by walls or other obstacles are in many situations sufficient to enforce this consistency. In addition, by intentionally walking according to consistent motion patterns for a limited period of time, the proposed algorithm enables calibration in e.g., outdoor areas where it may be difficult to set up infrastructure-dependent sensor systems.

Several extensions can be imagined. First, note that the estimation framework could just as well be used to calibrate other parameters than the zero-velocity detection threshold, such as the measurement variance for the zero-velocity updates. Similarly, the estimation framework could also be used to calibrate odometry based on other types of sensors, such as visual odometry. Second, it may possible to implement statistical tests that could answer questions such as “Does this fragment

of odometry comply with the assumptions of the FootSLAM algorithm?”, or “Has any of the underlying factors, such as gait mode or walking surface, changed to such an extent that the odometry needs to be recalibrated?”. By incorporating such tests into the proposed algorithm, a recalibration could be performed whenever it is possible *and* needed. When testing for changes in underlying factors, it may be useful to divide the data into non-overlapping windows, such that the FootSLAM algorithm converges using data from each separate window. Third, we mention the possibility of merging the proposed algorithm with one of the many proposed methods for adaptive thresholding using gait mode classification. Instead of learning a mapping between IMU-derived classification features and suitable thresholds using ground truth data, we could learn it using FootSLAM. This approach may enable a calibration algorithm that quickly adapts to changes in gait conditions (i.e., an algorithm that does not need to wait for convergence of the FootSLAM algorithm before each new recalibration) but which relies on the output from the FootSLAM algorithm to avoid dependence on ground truth data.

REFERENCES

- [1] R. Zhang, F. Hofflinger, and L. Reindl, “Inertial sensor based indoor localization and monitoring system for emergency responders,” *IEEE Sensors J.*, vol. 13, no. 2, pp. 838–848, Feb. 2013.
- [2] J. Wahlström, P. Porto Buarque de Gusmão, A. Markham, and N. Trigoni, “Map-aided navigation for emergency searches,” in *Proc. IEEE Int. Conf. Distrib. Comput. in Sensor Syst.*, Santorini Island, Greece, May 2019.
- [3] I. Skog, P. Händel, J. O. Nilsson, and J. Rantakokko, “Zero-velocity detection — An algorithm evaluation,” *IEEE Trans. Biomed. Eng.*, vol. 57, no. 11, pp. 2657–2666, Nov. 2010.
- [4] X. Tian, J. Chen, Y. Han, J. Shang, and N. Li, “A novel zero velocity interval detection algorithm for self-contained pedestrian navigation system with inertial sensors,” *Sensors*, vol. 16, no. 10, p. 1578, Jun. 2016.
- [5] S. Y. Park, H. Ju, and C. G. Park, “Stance phase detection of multiple actions for military drill using foot-mounted IMU,” in *Proc. IEEE Int. Conf. Indoor Positioning and Indoor Navigation*, Alcalá de Henares, Spain, Oct. 2016.
- [6] R. Zhang, H. Yang, F. Höflinger, and L. M. Reindl, “Adaptive zero velocity update based on velocity classification for pedestrian tracking,” *IEEE Sensors J.*, vol. 17, no. 7, pp. 2137–2145, Apr. 2017.
- [7] M. Ma, Q. Song, Y. Li, and Z. Zhou, “A zero velocity intervals detection algorithm based on sensor fusion for indoor pedestrian navigation,” in *Proc. IEEE Int. Conf. Inf. Technol., Netw., Electron. Autom. Control*, Chengdu, China, Dec. 2017, pp. 418–423.
- [8] B. Wagstaff, V. Peretroukhin, and J. Kelly, “Improving foot-mounted inertial navigation through real-time motion classification,” in *Proc. IEEE Int. Conf. Indoor Positioning and Indoor Navigation*, Sapporo, Japan, Sep. 2017.
- [9] B. Wagstaff, V. Peretroukhin, and J. Kelly, “Robust data-driven zero-velocity detection for foot-mounted inertial navigation,” *IEEE Sensors Journal*.
- [10] J. Wahlström, I. Skog, F. Gustafsson, A. Markham, and N. Trigoni, “Zero-velocity detection – a Bayesian approach to adaptive thresholding,” *IEEE Sensors Letters*, vol. 3, no. 6, Jun. 2019.
- [11] Y. Wang and A. M. Shkel, “Adaptive threshold for zero-velocity detector in ZUPT-aided pedestrian inertial navigation,” *IEEE Sensors Letters*.
- [12] H.-F. Liu, W. Ren, T. Zhang, J. Gong, J. m. Liang, B. Liu, J. w. Shi, and Z. Huang, “An adaptive selection algorithm of threshold value in zero velocity updating for personal navigation system,” in *Proc. 33rd Chinese Control Conf.*, Jul. 2014, pp. 1035–1038.
- [13] Q. Wang, Z. Guo, Z. Sun, X. Cui, and K. Liu, “Research on the forward and reverse calculation based on the adaptive zero-velocity interval adjustment for the foot-mounted inertial pedestrian-positioning system,” *Sensors*, vol. 18, no. 5, p. 1642, May 2018.
- [14] B. Wagstaff and J. Kelly, “LSTM-based zero-velocity detection for robust inertial navigation,” in *Proc. IEEE Int. Conf. Indoor Positioning and Indoor Navigation*, Nantes, France, Sep. 2018.
- [15] U. Walder and T. Bernoulli, “Context-adaptive algorithms to improve indoor positioning with inertial sensors,” in *Proc. IEEE Int. Conf. Indoor Positioning and Indoor Navigation*, Zurich, Switzerland, Sep. 2010.
- [16] M. Ren, K. Pan, Y. Liu, H. Guo, X. Zhang, and P. Wang, “A novel pedestrian navigation algorithm for a foot-mounted inertial-sensor-based system,” *Sensors*, vol. 16, no. 1, Jan. 2016.
- [17] Y. Li and J. J. Wang, “A robust pedestrian navigation algorithm with low cost IMU,” in *Proc. IEEE Int. Conf. Indoor Positioning and Indoor Navigation*, Sydney, Australia, Nov. 2012.
- [18] W. Sun, W. Ding, H. Yan, and S. Duan, “Zero velocity interval detection based on a continuous hidden Markov model in micro inertial pedestrian navigation,” *Meas. Sci. Technol.*, vol. 29, no. 6, Apr. 2018.
- [19] P. Robertson, M. Angermann, and B. Krach, “Simultaneous localization and mapping for pedestrians using only foot-mounted inertial sensors,” in *Proc. Int. Conf. Ubiquitous Comput.*, Orlando, FL, Sep. 2009, pp. 93–96.
- [20] M. García Puyol, D. Bobkov, P. Robertson, and T. Jost, “Pedestrian simultaneous localization and mapping in multistory buildings using inertial sensors,” *IEEE Trans. Intell. Transp. Syst.*, vol. 15, no. 4, pp. 1714–1727, Aug. 2014.
- [21] M. García Puyol, “Merging of maps obtained with human odometry based on FootSLAM for pedestrian navigation,” Master’s thesis, University of Malaga, Sep. 2011.
- [22] P. Robertson, M. Frassl, M. Angermann, M. Doniec, B. J. Julian, M. García Puyol, M. Khider, M. Lichtenstern, and L. Bruno, “Simultaneous localization and mapping for pedestrians using distortions of the local magnetic field intensity in large indoor environments,” in *Proc. IEEE Int. Conf. Indoor Positioning and Indoor Navigation*, Montbeliard-Belfort, France, Oct. 2013.
- [23] M. Angermann and P. Robertson, “FootSLAM: Pedestrian simultaneous localization and mapping without exteroceptive sensors – hitchhiking on human perception and cognition,” *Proc. IEEE*, vol. 100, no. Special Centennial Issue, pp. 1840–1848, May 2012.
- [24] S. Kaiser and C. Lang, “Integrating moving platforms in a SLAM algorithm for pedestrian navigation,” *Sensors*, vol. 18, no. 12, Dec. 2018.
- [25] J. Olsson and T. Rydén, “Asymptotic properties of particle filter-based maximum likelihood estimators for state space models,” *Stochastic Processes and their Appl.*, vol. 118, no. 4, pp. 649–680, Apr. 2008.
- [26] D. S. Colomar, J. Nilsson, and P. Händel, “Smoothing for ZUPT-aided INSs,” in *Proc. IEEE Int. Conf. Indoor Positioning and Indoor Navigation*, Sydney, Australia, Nov. 2012.
- [27] J. D. Hol, T. B. Schön, and F. Gustafsson, “On resampling algorithms for particle filters,” in *Proc. IEEE Nonlinear Statistical Signal Process. Workshop*, Cambridge, UK, Sep. 2006, pp. 79–82.